

Supplementary Materials: Comparative Analyses between the Zero-Inertia and Fully Dynamic Models of the Shallow Water Equations for Unsteady Overland Flow Propagation

Costanza Aricò * and Carmelo Nasello

Part A: The numerical procedures

A.1 The fractional time step procedure

The two numerical models applied in this paper are based on a time-splitting approach, where a prediction and a correction problem are sequentially solved. For both the numerical procedures, it has been shown that the prediction and the correction steps have the characteristics of a convective and a diffusive problem, respectively [2–5]. For these reasons, we call the prediction system "convective prediction" (CP) system and the correction system "diffusive correction" (DC) system.

Let's assume a general system of balance laws,

$$\frac{\partial \mathbf{U}}{\partial t} + \nabla \cdot \mathbf{F}(\mathbf{U}) = \mathbf{B}(\mathbf{U}) \quad \text{A.1}$$

where \mathbf{U} , $\mathbf{F}(\mathbf{U})$ and $\mathbf{B}(\mathbf{U})$ are the vector of the unknown variables, the flux vector and the source term respectively. Let $\mathbf{F}^p(\mathbf{U})$ and $\mathbf{B}^p(\mathbf{U})$ be a suitable numerical flux and source term respectively, further defined, applying a fractional time-step procedure, we set:

$$\mathbf{F}(\mathbf{U}) = \mathbf{F}^p(\mathbf{U}) + (\mathbf{F}(\mathbf{U}) - \mathbf{F}^p(\mathbf{U})) \quad \text{A.2,a}$$

$$\mathbf{B}(\mathbf{U}) = \mathbf{B}^p(\mathbf{U}) + (\mathbf{B}(\mathbf{U}) - \mathbf{B}^p(\mathbf{U})) \quad \text{A.2,b}$$

Applying integration in time, we split system (A.1) in the two following ones:

$$\mathbf{U}^{k+1/2} - \mathbf{U}^k + \nabla \cdot \int_0^{\Delta t} \mathbf{F}^p dt = \int_0^{\Delta t} \mathbf{B}^p dt \quad \text{A.3,a}$$

$$\mathbf{U}^{k+1} - \mathbf{U}^{k+1/2} + \nabla \cdot \int_0^{\Delta t} \mathbf{F} dt - \nabla \cdot \bar{\mathbf{F}}^p \Delta t = \int_0^{\Delta t} \mathbf{B} dt - \bar{\mathbf{B}}^p \Delta t \quad \text{A.3,b}$$

and we call systems (A.3,a) and (A.3,b) prediction and correction systems respectively. In Eqs (A.3), the overbar symbol marks the mean in time values of the numerical flux and source terms computed during the prediction step and apices k , $k+1/2$ and $k+1$ mark the values of the unknown variables computed at the beginning of the time step, at the end of the prediction step and at the end of the correction step respectively. The integrals $\bar{\mathbf{F}}^p \Delta t$ and $\bar{\mathbf{B}}^p \Delta t$ in Eq. (A.3,b) are computed "a posteriori" after the solution of the prediction problem, as explained in [2,3,5] for the fully dynamic model and in [4] for the diffusive model, respectively. Observe that summing systems (A.3,a) and (A.3,b), the integral of the original system (A.1) is formally obtained. The difference $(\mathbf{U}^{k+1} - \mathbf{U}^{k+1/2})$ in Eq. (A.3,b) is close to zero as far as the differences of the flux terms integrals $\left(\nabla \cdot \int_0^{\Delta t} \mathbf{F} dt - \nabla \cdot \bar{\mathbf{F}}^p \Delta t \right)$ and

of the source terms $\left(\int_0^{\Delta t} \mathbf{B} dt - \bar{\mathbf{B}}^p \Delta t \right)$, respectively on the l.h.s. and r.h.s. in the same equation, are small.

A suitable choice of terms $\mathbf{F}^p(\mathbf{U})$ and $\mathbf{B}^p(\mathbf{U})$ in the prediction step allows a much easier solution of the two steps in Eqs. (A.3) with respect to the original formulation in system (A.1).

In the FDSWEsM, vectors \mathbf{U} , $\mathbf{F}(\mathbf{U})$ and $\mathbf{B}(\mathbf{U})$ have the following expressions:

$$\mathbf{U} = (h \quad uh \quad vh)^T \quad \mathbf{F} = (\mathbf{F}_1 \quad \mathbf{F}_2)$$

$$\mathbf{F}_1 = \begin{pmatrix} uh \\ u^2h + \frac{1}{2}gh^2 \\ uvh \end{pmatrix} \quad \mathbf{F}_2 = \begin{pmatrix} vh \\ v^2h + \frac{1}{2}gh^2 \\ uvh \end{pmatrix} \tag{A.4,a}$$

$$\mathbf{B} = \left(p \quad -gh \left(\frac{\partial z}{\partial x} + \frac{n^2 u \sqrt{(uh)^2 + (vh)^2}}{h^{7/3}} \right) \quad -gh \left(\frac{\partial z}{\partial y} + \frac{n^2 v \sqrt{(uh)^2 + (vh)^2}}{h^{7/3}} \right) \right)^T$$

$$\mathbf{F}_1^p = \begin{pmatrix} uh \\ u^2h \\ uvh \end{pmatrix} \quad \mathbf{F}_2^p = \begin{pmatrix} vh \\ v^2h \\ uvh \end{pmatrix}$$

$$\mathbf{B}^p = \left(p \quad -gh \left(\frac{\partial H^k}{\partial x} + \frac{n^2 u \sqrt{(uh)^2 + (vh)^2}}{h^{7/3}} \right) \quad -gh \left(\frac{\partial H^k}{\partial y} + \frac{n^2 v \sqrt{(uh)^2 + (vh)^2}}{h^{7/3}} \right) \right)^T \tag{A.4,b}$$

where $(.)^T$ is the transposed of vector $(.)$.

In the 0ISWEsM, the same vectors assume the following forms:

$$\mathbf{U} = H \quad \mathbf{F} = -\frac{h^{5/3}}{n\sqrt{|\nabla H|}} \nabla H \quad \mathbf{B} = p \tag{A.5,a}$$

$$\mathbf{F}^p = -\frac{h^{5/3}}{n\sqrt{|\nabla H|^k}} (\nabla H)^k, \quad \mathbf{B}^p = \mathbf{B} \tag{A.5,b}$$

In both the FDSWEsM and 0ISWEsM, the gradients of the water level in the prediction step are computed at time level t^k and are kept constant during the time step (in the source term vector \mathbf{B}^p and in the flux term \mathbf{F}^p , respectively for the FDSWEsM and 0ISWEsM. More details in [2-5].

A.2. Spatial integration of the governing equations

In both the numerical solvers, the governing equations are integrated over unstructured triangular meshes satisfying the Generalized Delaunay (GD) property [4]. Let T_h be an unstructured GD triangulation of the 2D bounded domain Ω . We call *basic mesh* the triangulation T_h with N_T triangles and N nodes and its generic triangle and node are denoted as k_T and P_i ($i = 1, \dots, N$), respectively. We construct a *dual mesh* E_h over the basic mesh and its dual element (or dual finite volume), associated with the node P_i , is denoted as e_i ($i = 1, \dots, N$). This is the closed region obtained by merging the sub-triangles given by subdividing each triangle k_T sharing node P_i , by means of its axes (see figure 1). e_i is the Voronoi region (or Voronoi polygon) ([4] and cited references).

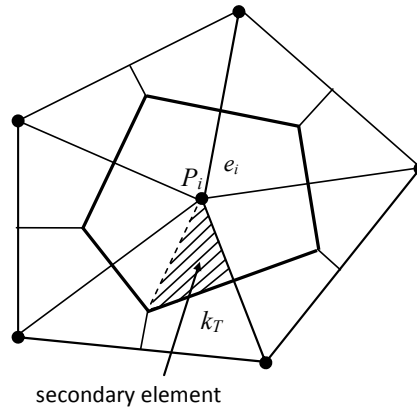


Figure S1. The basic and the dual mesh.

A.3. The numerical solution of the OISWEsM

In the OISWEsM [4], the computational cell is the Voronoi polygon e_i and the storage capacity is concentrated in the node P_i in the measure of $1/3$ of the area of all the triangles sharing P_i . The authors in [4] assume a linear variation of the water level H inside each triangle, according to the three nodal values.

In the OISWEs physical problem, the flow field has an exact scalar potential, that is the water level. For the application of the MAST procedure, at the beginning of each time step, the cells are ordered on the base of their potential values, computed at the end of the previous time step or, for the first time iteration, given by the initial condition.

According to Eqs. (4), (A.2)-(A.3) and (A.5), after integration in space and application of the Green theorem, the integral form of the CP system for the generic computational cell i is [4]

$$A_i \frac{dH_i}{dt} + \sum_j FL_{i,j}^{out} = \sum_m FL_{i,m}^{in} + A_i p_i, \text{ with, } FL_{i,j}^{out} = K_{i,j}^k h_i^{5/3}, \quad A_i = \frac{1}{3} \sum_{n=1, N_T} |k_{T_n}| \delta_{i,n}, \quad i=1, \dots, N \tag{A.6}$$

where A_i is the area of cell i , $|k_{T_n}|$ is the area of triangle n , $\delta_{i,n}$ is equal to 1 if triangle n shares node i , 0 otherwise, $FL_{i,j}^{out}$ is the flux leaving cell i to the any neighbouring downstream (in the potential scale) cell j (with $H_j^k \leq H_i^k$), $K_{i,j}^k$ is the flux coefficient, further defined, $FL_{i,m}^{in}$ is the flux entering cell i from any neighbouring upstream (in the potential scale) cell m with $H_i^k \leq H_m^k$ and p_i is source term in node i . The flux coefficient is defined as (see Eqs.(19)-(22) in [4])

$$K_{i,j}^k = (c_{i,j}^1 E_1^k + c_{i,j}^2 E_2^k) \frac{(H_i^k - H_j^k)}{d_{ij}} \tag{A.7}$$

where d_{ij} is the distance between nodes i and j , indices 1 and 2 mark the two triangles sharing side ij , the coefficient $E_{1(2)}^k$ is

$$E_m^k = \frac{1}{n_m \sqrt{|\nabla H_m^k|}}, \quad m = 1, 2 \tag{A.8}$$

where the sub-index m marks all the parameters of the triangle m sharing the same side and $c_{i,j}^{1(2)}$ is the distance between the midpoint of side ij and the circumcentre of triangle m . If side ij shares only one triangle, $c_{i,j}^2$ and E_2^k are zero. The distance $c_{i,j}^{1(2)}$ is computed as in Eqs. (19) in [4], where the

authors prove that the proposed formulation guarantees the consistency of the flux between cells i and j and the difference of the corresponding potentials $(H_i^k - H_j^k)$ for an unstructured GD mesh.

If the r.h.s. of system (A.6) is approximated with its mean value in the time step, the solution of the same system is disentangled in the sequential solution of N Ordinary Differential Equations (ODEs) [4],

$$A_i \frac{dH_i}{dt} + \sum_j F_{i,j}^{out} = \sum_m \overline{F}_{i,m}^{in} + A_i \overline{p}_i \quad \text{A.9}$$

one for each cell, going from the cell with highest to the cell with the lowest potential value. In Eq. (A.9), $\overline{F}_{i,m}^{in}$ is the mean in time value of the flux entering from the upstream (in the potential scale) cell m , previously solved, and \overline{p}_i is the mean (in time) value of p_i . A very fast semi-analytical solution of the ODEs (A.9) is proposed in [4], which allows to save a lot of computational time.

Call h_i^k the water depth at the beginning of the time step and h_i^{kf} its asymptotic steady-state value (i. e. when $dH_i/dt=0$), computed according to Eqs. (A.9),

$$h_i^{kf} = \left(\frac{\overline{F}_i^{in}}{\sum_j K_{i,j}^k} \right)^{3/5}, \quad \text{with } \overline{F}_i^{in} = \overline{F}_{i,m}^{in} + A_i \overline{p}_i \quad \text{A.10}$$

Eq. (A.9) can be written in dimensionless form as:

$$\frac{d\xi}{d\tau} = 1 - \xi^{5/3}, \quad \xi = \frac{h_i}{h_i^{kf}}, \quad \tau = \frac{dt \overline{F}_i^{in}}{A_i h_i^{kf}}, \quad \text{if } h_i^{kf} > h_i^k \quad \text{A.11,a}$$

$$\frac{d\xi}{d\tau} = \xi_f^{5/3} - \xi^{5/3}, \quad \xi = \frac{h_i}{h_i^k}, \quad \tau = \frac{dt \overline{F}_i^{in}}{A_i h_i^k} \left(\frac{h_i^k}{h_i^{kf}} \right)^{5/3}, \quad \text{if } h_i^{kf} < h_i^k \quad \text{A.11,b}$$

The proposed semi-analytical solution proposed in [4] is

$$\xi = \frac{\exp(c_1 \tau) + c_2}{\exp(c_1 \tau) + c_3} \quad \text{if } h_i^{kf} > h_i^k \quad \text{A.12,a}$$

$$\xi = 1 + (\xi_f - 1) \frac{\exp(c_1 \tau) + c_2}{\exp(c_1 \tau) + c_3} \quad \text{if } h_i^{kf} < h_i^k \quad \text{A.12,b}$$

with a proper choice of the c_1 , c_2 and c_3 coefficients. Using any c_3 value it is possible to match the initial value ξ_0 and its first derivative ξ_0' by setting:

$$c_2 = \xi_0 (1 + c_3) - 1, \quad c_1 = \xi_0' \frac{(1 + c_3)^2}{(c_3 - c_2)} \quad \text{if } h_i^{kf} > h_i^k \quad \text{A.13,a}$$

$$c_2 = -1, \quad c_1 = \xi_0' \frac{(1 + c_3)}{(\xi_f - 1)} \quad \text{if } h_i^{kf} < h_i^k \quad \text{A.13,b}$$

The c_3 coefficient affects the maximum error that is obtained according to functions (A.12) using different time step sizes. This optimum depends on ξ_0 , if $h_i^{kf} > h_i^k$ and on ξ_f , if $h_i^{kf} < h_i^k$. The optimum coefficients have been computed numerically for different possible ξ_0 and ξ_f values by comparing functions (A.12) with a numerical solution computed using a very small time step. See in table 1 and in figure 7 in [4] the computed optimum c_3 values. See in figures 8,a and 8,b in [4] the

numerical solution of Eqs. (A.11) in the case of respectively $\xi_0 = 0$ and $\xi_f = 0$, compared with the semi-analytical solutions (A.12) corresponding to the optimal c_3 values (respectively 0.7469 and -0.8171). The maximum error computed with the initial conditions $\xi_0 = 0$, for $h_i^{kf} > h_i^k$, or $\xi_f = 0$, for $h_i^{kf} < h_i^k$, is the worse one and it is smaller than 10^{-3} . More details can be found in [4]

After the solution of each ODEs (A.9), the mean in time total flux going from cell i to the neighbouring downstream (in the potential scale) cells is computed applying the local mass balance for cell i [4]. In the framework of the MAST procedure, due to the sequential solution of the cells and their ordering at the beginning of the time iteration, the mean (in time) entering flux is always known before each solution of the ODEs (A.9) [4].

The same spatial discretization adopted for the CP problem is used in the DC problem and the initial condition of the DC problem is the final state obtained after the solution of the CP step, marked with the index $k+1/2$. Starting from Eqs. (4), (A.2)-(A.3) and (A.5), after spatial integration of the correction problem inside each Voronoi cell, the following DC system is obtained [4]

$$\frac{A_i}{\Delta t} \eta_i + \sum_{n=1, N_T} D_{i,j}^k (\eta_i - \eta_j) \delta_{i,n} = \sum_{n=1, N_T} D_{i,j}^k (\vartheta_j - \vartheta_i) \delta_{i,n} \quad i = 1, \dots, N \quad \text{A.14,a}$$

where

$$\eta = H - H^{k+1/2}, \quad \vartheta = H^k - H^{k+1/2}, \quad D_{i,j}^k = \sum_{m=1,2} \frac{c_{i,j}^m E_m^k}{d_{ij}} (h_l^{km})^{5/3}, \quad \text{A.14,b}$$

$$h^{km} = \frac{h^k + h^{k+1/2}}{2}$$

with initial condition $\eta = 0$. In Eq. (A.14,a), $\delta_{i,n}$ has been previously specified and the sum in Eq. (A.14,b) is extended to the two triangles m sharing side ij . $l = i$ if $H_i^k \geq H_j^k$, $l = j$ if $H_i^k < H_j^k$. The proposed formulation of the coefficients $D_{i,j}^k$ provides the same flux estimation of the CP step [4] and it is similar to the one of a standard linear (P1) Finite Element Galerkin scheme. Analogies and differences between the flux formulation adopted in the present DSWEs model and the one of a P1 Galerkin scheme are presented and discussed for a GD triangulation in [4].

The matrix of the linear system resulting from Eqs. (A.14) has order N (the number of the nodes) and, in the case of a GD triangulation, it is symmetric, positive-definite, strictly diagonally dominant, with M -property and system (A.14) is well-conditioned [4]. After the unknowns are computed by solving the system (A.14), the final values of the water levels are updated as

$$H^{k+1} = H^{k+1/2} + \eta; \quad \text{A.15}$$

The splitting of the original governing equations in the CP and DC steps, allows this 0ISWEsM solver to easily deal with waves/flooding propagation problems over dry domains, as well as a robust solution of wetting/drying problems [4].

A.3.1. Investigation of the behaviour of the proposed 0ISWEsM over refined meshes and smooth surfaces

If the area A_i of the i^{th} Voronoi cell goes approaches zero, the dimensionless variable η in Eqs. (A.11) approaches infinity, and the solution of the prediction step is given to the asymptotic values in Eqs. (A.12,a) or (A.12,b), respectively if $h_i^{kf} > h_i^k$ or $h_i^{kf} < h_i^k$, shown in figures 8 in [4].

In the correction step, the value of the capacity term $A_i / \Delta t$ in system (A.14) becomes negligible compared with the flux terms $\sum_{n=1, N_T} D_{i,j}^k (\eta_i - \eta_j) \delta_{i,n}$ and $\sum_{n=1, N_T} D_{i,j}^k (\vartheta_j - \vartheta_i) \delta_{i,n}$

If the Manning coefficient n approaches zero, coefficient E_m^k in Eq. (A.8) approaches infinity, as well as the flux coefficient in the prediction step $K_{i,j}^k$ in Eq. (A.7) and $\sum_j K_{i,j}^k$ in Eq. (A.10).

This implies that the asymptotic steady-state value h_i^{kf} in Eq. (A.10) approaches zero and the dimensionless variable ξ in Eqs. (A.11) approaches infinity. In this case, the dimensionless solution ξ of the semi-analytical procedure of the prediction step is given by the asymptotic value of Eq. (A.12,b).

Coefficient $D_{i,j}^k$ in the correction system in Eq. (A.14,a) approaches infinity (see the third of Eq. (A.14,b)). By dividing the terms in Eq. (A.14,a) by coefficient $D_{i,j}^k$, the capacity term becomes negligible with respect to the other terms in the same equation.

A.3.2. Preservation of the water at rest condition (C-property)

The proposed 0ISWEsM preserves the C-property (e.g., [7]). For quiescent water, we have, in the prediction step, zero flux entering in each cell and zero gradient of the water level H . This implies that in Eq. (A.6) we have $\sum_m F_{i,m}^{in} = 0$ and, from Eqs. (A.7)-(A.8) $\sum_j F_{i,j}^{out} = 0$. The solution of the prediction step gives $H^{k+1/2} = H^k$. System (A.14) in the correction step becomes

$$\frac{A_i}{\Delta t} \eta_i + \sum_{n=1, N_T} D_{i,j}^k (\eta_i - \eta_j) \delta_{i,n} = 0 \tag{A.16}$$

since $\vartheta = H^k - H^{k+1/2} = 0$, and this implies that the correction of the water level η_i is zero.

A.4. The numerical solution of the FDSWEsM

In the FDSWEsM, the computational cell is the triangle k_T , with the storage capacity concentrated in the circumcentre of k_T in the measure of the area of k_T and a piecewise constant value of the unknown variables h (as well as H), uh and vh is assumed inside each triangle [3, 5].

According to Eqs. (1)-(2), (A.2)-(A.4), by integrating in space the prediction problem and applying the Green's theorem, the integral form of the CP system is [3, 5]

$$\frac{\partial h}{\partial t} |k_T|_e + \sum_{j=1,3} \delta_{j,e} F_{j,e}^{out} = \sum_{j=1,3} (1 - \delta_{j,e}) F_{j,e}^{in} + |k_T|_e p_e \quad e = 1, \dots, N_T \tag{A.17}$$

$$\frac{\partial q_{s,e}}{\partial t} |k_T|_e + \sum_{j=1,3} \delta_{j,e} M_{j,e}^{s,out} + R_e^s = \sum_{j=1,3} (1 - \delta_{j,e}) M_{j,e}^{s,in}, \quad \text{with } s = x, y, \tag{A.18}$$

$$q_s = \begin{cases} uh & \text{if } s=x \\ vh & \text{if } s=y \end{cases}$$

where index e marks the values of the variables in triangle $k_{T,e}$, $F_{j,e}^{out(in)}$ and $M_{j,e}^{x(y)out(in)}$ are the flux and the $x(y)$ component of the momentum flux, leaving (entering) cell $k_{T,e}$ across side j ($j = 1, 2, 3$) of $k_{T,e}$, respectively, $\delta_{j,e} = 1$ (0) if the flux across side j of $k_{T,e}$ is oriented outward (inward) $k_{T,e}$, p_e is the source term in cell $k_{T,e}$ and $R_e^{x(y)}$ is the source term defined as [3],

$$R_e^s = bfr_e^s + gr_e^s \quad \text{with } bfr_e^s = |k_T|_e g \frac{n^2 q_{s,e} \sqrt{(uh)_e^2 + (vh)_e^2}}{h_e^{7/3}} \quad \text{and} \tag{A.19}$$

$$gr_e^s = |k_T|_e g h_e \frac{\partial H_e^k}{\partial s}$$

The first term on the l.h.s. of Eq. (A.18) is the integral form of the local inertia (or local acceleration), the two summations of the same equation, on the l.h.s. and r.h.s., respectively, represent the integral form of the convective inertia (or convective acceleration), computed as the line integral of the momentum fluxes across the sides of the computational cell, the third term on the l.h.s of Eq.

(A.18), is the sum of the integral form of the bottom friction bfr_e^s and water level gradient gr_e^s terms.

As for the OISWEs problem, the authors in [3,5] disentangle the solution of the prediction system in Eqs. (A.17)–(A.18) in the sequential solution of N_T ODEs, by approximating the r.h.s. of the same equations with their mean values in time computed during the time step.

To apply the sequential solution of the computational cells, it is necessary to order them [3,5], but, unlike the previous DSWEs problem, an exact scalar potential of the flow field does not exist in the FDSWEs physical problem. For this reason, the authors in [2,3,6] add a convective corrective (CC) step, splitting the original prediction step in a "convective prediction" (CP) system and in a "convective correction" (CC) system [3,6].

The computational cells are ordered by applying an iterative procedure based on the inter-cell flux direction between adjacent cells, proposed in [5] and further modified in [6]. In the following, we call no_e^k the order number of cell $k_{T,e}$ at the beginning of the generic time step (time level t^k).

After the ordering of the computational cells, the CP step is solved as a sequence of small systems of ODEs, from time level t^k to time level $t^k + \Delta t$ [5], proceeding from the cell(s) with the lowest no_e^k value to the cell(s) with the highest no_e^k value. The same procedure is repeated in the CC step, proceeding in the opposite direction, from the cell(s) with the highest to the cell(s) with the lowest no_e^k value [6]. Cell $k_{T,e}$ with order no_e^k is solved only after the solution of the neighbouring $k_{T,ep}$ cells with $no_{ep}^k < no_e^k$ ($no_{ep}^k > no_e^k$), in the CP (CC) step [5]. The ODEs system of the CP problem is [3, 5]

$$\frac{dh_e}{dt} |k_{T,e}| + \frac{1}{\Delta t} \int \sum_{j=1,3} \delta_{j,e} F_{j,e}^{p,out}(t) dt = \sum_{j=1,3} (1 - \delta_{j,e}) \bar{F}_{j,e}^{p,in} + |k_{T,e}| \bar{p}_e, e = 1, \dots, N_T \quad A.20$$

$$\begin{aligned} \frac{dq_{s,e}}{dt} |k_{T,e}| + \frac{1}{\Delta t} \int R_e^s(t) dt + \frac{1}{\Delta t} \int \sum_{j=1,3} \delta_{j,e} M_{j,e}^{p,s,out}(t) dt &= \sum_{j=1,3} (1 - \delta_{j,e}) \bar{M}_{j,e}^{p,s,in} \quad s \\ &= x, y \end{aligned} \quad A.21$$

with the symbols specified as above and the leaving flux and momentum flux $F_{j,e}^{p,out}$ and $M_{j,e}^{p,x(y),out}$ defined as follows. If the two neighbouring triangles $k_{T,e}$ and $k_{T,ep}$ share side $r_{i,ip}$ between nodes i and ip , where $r_{i,ip}$ is the j^{th} side of $k_{T,e}$ and the m^{th} side of $k_{T,ep}$ ($j, m = 1, 2, 3$), we define the flux across side j of $k_{T,e}$ as [3]

$$FL_{j,e} = (uh)_e (y_{ip} - y_i) - (vh)_e (x_{ip} - x_i) \quad A.22$$

and the flux and the momentum fluxes between $k_{T,e}$ and $k_{T,ep}$ as [3]

$$F_{j,e} = FL_{j,e} \quad \text{if} \quad FL_{j,e} > 0 \quad \text{and} \quad FL_{j,e} > FL_{m,ep} \quad A.23,a$$

$$F_{j,e} = -FL_{m,ep} \quad \text{otherwise} \quad A.23,b$$

$$M_{j,e}^x = F_{j,e} \frac{(uh)_e}{h_e}, \quad M_{j,e}^y = F_{j,e} \frac{(vh)_e}{h_e} \quad \text{if} \quad F_{j,e} = FL_{j,e} \quad A.24,a$$

$$M_{j,e}^x = F_{j,e} \frac{(uh)_{ep}}{h_{ep}}, \quad M_{j,e}^y = F_{j,e} \frac{(vh)_{ep}}{h_{ep}} \quad \text{otherwise} \quad A.24,b$$

Flux/momentum flux continuity is guaranteed at each triangle side by Equations (A.23)–(A.24) and $F_{j,e} = -F_{m,ep}$ and $M_{j,e}^{x(y)} = -M_{m,ep}^{x(y)}$.

The leaving flux/momentum flux $F_{j,e}^{p,out}$ and $M_{j,e}^{p,x(y),out}$ in Eqs. (A.20)–(A.21) of the CP step, going from cell $k_{T,e}$ to the neighbouring cell $k_{T,ep}$ (with $no_e^k < no_{ep}^k$), are defined as [3]

$$F_{j,e}^{p,out} = \max\left(0, F_{j,e}\right), \quad M_{j,e}^{p,x,out} = F_{j,e}^{p,out} \frac{(uh)_e}{h_e}, \quad M_{j,e}^{p,y,out} = F_{j,e}^{p,out} \frac{(vh)_e}{h_e} \quad \text{if} \quad \text{A.25,b}$$

$$no_e^k < no_{ep}^k \quad (\text{A.25,a}), \quad F_{j,e}^{p,out} = M_{j,e}^{p,x(y),out} = 0 \quad \text{if} \quad no_e^k > no_{ep}^k$$

$\bar{F}_{j,e}^{p,in}$ and $\bar{M}_{j,e}^{p,s,in}$ on the r.h.s. of Eqs. (A.20)–(A.21) are the mean in time values of the incoming fluxes and momentum fluxes, respectively (know from the solution of the previously solved neighbouring $k_{T,ep}$ cells with $no_e^k > no_{ep}^k$ [2, 3, 5, 6]) and \bar{p}_e is the mean in time value of the source term in $k_{T,e}$.

Once the ODEs system (A.20)–(A.21) is solved for $k_{T,e}$, the mean in time value of the total flux \bar{F}_e^{out} leaving from $k_{T,e}$, from t^k to $t^k + \Delta t$, is computed according to the local mass balance for cell $k_{T,e}$ [3]. The mean in time flux $\bar{F}_{j,e}^{out}$ and momentum fluxes $\bar{M}_{j,e}^{x(y),out}$, leaving from the j^{th} side of $k_{T,e}$ to the m^{th} side of the neighbouring cell $k_{T,ep}$ (with $no_e^k < no_{ep}^k$) are estimated as in [2, 3, 5]. After that, the same ODEs system (A.20)–(A.21) is solved for cell $k_{T,ep}$, selected among the unsolved ones according to

$$no_{ep}^k > no_e^k \quad \text{and} \quad no_{ep}^k = \min(no_{el}^k), \quad k_{T,el} \subset \text{set of unsolved cells} \quad \text{A.26}$$

The same procedure is applied for the solution of the CC step, whose ODEs system is

$$\frac{dh_e}{dt} |T_e| + \frac{1}{\Delta t} \int \sum_{j=1,3} \delta_{j,e} F_{j,e}^{c,out}(t) dt = \sum_{j=1,3} (1 - \delta_{j,e}) \bar{F}_{j,e}^{c,in} \quad \text{A.27}$$

$$\frac{dq_{s,e}}{dt} |T_i| + \frac{1}{\Delta t} \int \sum_{j=1,3} \delta_{j,e} M_{j,e}^{c,s,out}(t) dt = \sum_{j=1,3} (1 - \delta_{j,e}) \bar{M}_{j,e}^{c,s,in}, \quad s = x, y \quad \text{A.28}$$

with $\delta_{j,e}$ defined as above and the leaving flux/momentum flux $F_{j,e}^{c,out}$ and $M_{j,e}^{c,x(y),out}$ in Eq. (A.27)–(A.28) of the CC step, going from cell $k_{T,e}$ to the neighbouring cell $k_{T,ep}$ (with $no_e^k > no_{ep}^k$), are defined as [3]

$$F_{j,e}^{c,out} = \max\left(0, F_{j,e}\right), \quad M_{j,e}^{c,x,out} = F_{j,e}^{c,out} \frac{(uh)_e}{h_e}, \quad M_{j,e}^{c,y,out} = F_{j,e}^{c,out} \frac{(vh)_e}{h_e} \quad \text{if}$$

$$no_e^k > no_{ep}^k \quad (\text{A.29,a}), \quad F_{j,e}^{c,out} = M_{j,e}^{c,x(y),out} = 0 \quad \text{if} \quad \text{A.29,b}$$

$$no_e^k < no_{ep}^k$$

As motivated in [2, 3], the source terms are allocated in the CP step.

After the solution of the ODEs system (A.27)–(A.28) for cell $k_{T,e}$, the total leaving fluxes/momentum fluxes from side j of $k_{T,e}$ to the neighbouring cell $k_{T,ep}$ with $no_e^k > no_{ep}^k$ are computed as for the previous CP step. More details in [2,3,6].

According to Equations (1)–(2), (A.2)–(A.4), after integration in space, neglecting the inertial terms in the momentum equations (as motivated in [2,3]), substituting the momentum equations in the continuity equation and applying the Green's theorem, we obtain a linearized system in the unknown water level [2,3,5],

$$\int_{k_{T,e}} \frac{\partial H}{\partial t} dk_{T,e} + \sum_{j=1,3} \int_{L_{j,e}} -elem_e \frac{\partial H^{k+1}}{\partial n_{j,e}} dl = \sum_{j=1,3} \int_{L_{j,e}} -elem_e \frac{\partial H^k}{\partial n_{j,e}} dl + \sum_{j=1,3} \int_{L_{j,e}} (\bar{\mathbf{q}} - \mathbf{q}^{cc}) \cdot \hat{\mathbf{n}}_{j,e} dl \quad \text{A.30,a}$$

$$\text{with } elem_e = g\bar{h}_e \Delta t / \left(1 + \Delta t g n^2 \left(\frac{\sqrt{(uh)_e^2 + (vh)_e^2}}{h_e^{7/3}} \right) \right) \quad \text{and } e = 1, \dots, N_T \quad \text{A.30,b}$$

where $L_{j,e}$ is the length of side j of triangle $k_{T,e}$, $\hat{\mathbf{n}}_{j,e}$ is its unit orthogonal vector, $\bar{\mathbf{q}}$ and \mathbf{q}^{cc} are the mean in time value of the flow rate vector computed during the (CP + CC) steps and its final value, respectively [Error! Reference source not found.] and symbols $(\bar{*})$ in Eq. (A.30) is the mean in time value of $(*)$ computed during the (CP + CC) steps. The initial state for the DC step is the solution computed at the end of the CC step. The matrix of the linear system resulting from Eqs. (A.30) has order N_T (the number of the triangles) and, in the case of a GD triangulation, is well conditioned, symmetric, positive-definite, strictly diagonally dominant, with M -property and system (A.30) is well-conditioned [5]. After solving the DC step, uh and vh are updated, as well as the spatial gradients of the water levels, as explained in [5].

Part B. Supplementary material for the presented tests

In this Appendix we plot the figures and tables recalled in the text of the main paper.

Test 1. Steady flow in a 1D channel with undulating bottom profile

OISWEsM								FDSWEsM							
r_c	$L_{1,h}$	r_c	$L_{1,uh}$	r_c	$L_{2,h}$	r_c	$L_{2,uh}$	r_c	$L_{1,h}$	r_c	$L_{1,uh}$	r_c	$L_{2,h}$	r_c	$L_{2,uh}$
case 1								case 1							
0.323	0.0311	0.350	0.0031	0.384	0.0526	0.348	0.0053	0.949	0.0036	0.987	0.0023	0.996	0.0059	0.907	0.0049
0.520	0.0248	0.464	0.0024	0.481	0.0403	0.496	0.0042	1.055	0.0019	1.059	0.0011	1.030	0.0030	0.927	0.0026
0.615	0.0173	0.660	0.0017	0.597	0.0289	0.577	0.0030	1.065	0.0009	1.026	0.0006	1.012	0.0015	1.077	0.0014
	0.0113		0.0011		0.019		0.0020		0.0004		0.0003		0.0007		0.0006
case 2								case 2							
0.712	0.0070	0.502	0.0028	0.799	0.0126	0.476	0.0041	0.971	0.0036	0.994	0.0023	0.948	0.0060	0.963	0.0049
0.817	0.0043	0.634	0.0020	0.844	0.0073	0.694	0.0029	1.047	0.0019	1.089	0.0011	1.050	0.0031	1.048	0.0025
0.991	0.0024	0.876	0.0013	1.083	0.0040	0.807	0.0018	1.103	0.0009	1.030	0.0005	1.001	0.0015	1.007	0.0012
	0.0012		0.0007		0.0019		0.0010		0.0004		0.0003		0.0007		0.0006
case 3								case 3							
0.967	0.0039	0.520	0.0028	0.890	0.0065	0.554	0.0039	0.940	0.0043	0.940	0.0009	0.932	0.0076	0.893	0.0016
1.012	0.0020	0.657	0.0019	0.959	0.0035	0.777	0.0026	1.059	0.0022	1.056	0.0005	1.000	0.0040	0.981	0.0008
1.032	0.0010	0.836	0.0012	1.016	0.0018	0.895	0.0015	1.051	0.0011	1.070	0.0002	1.029	0.0020	1.104	0.0004
	0.0005		0.0007		0.0009		0.0008		0.0005		0.0001		0.0010		0.0002
case 4								case 4							
0.951	0.0039	0.582	0.0026	0.905	0.0065	0.584	0.0037	0.913	0.0043	1.000	0.0009	0.858	0.0076	0.976	0.0016
0.998	0.0020	0.772	0.0017	0.956	0.0035	0.823	0.0025	0.987	0.0023	1.106	0.0005	1.066	0.0042	1.074	0.0008
1.005	0.0010	1.008	0.0010	0.983	0.0018	0.926	0.0014	1.082	0.0011	1.064	0.0002	1.004	0.0020	1.078	0.0004
	0.0005		0.0005		0.0009		0.0007		0.0005		0.0001		0.0010		0.0002

Figure S1. Test 1. L_1 and L_2 norms of the relative errors for h and uh . Unstructured meshes.

OISWEsM								FDSWEsM							
r_c	$L_{1,h}$	r_c	$L_{1,uh}$	r_c	$L_{2,h}$	r_c	$L_{2,uh}$	r_c	$L_{1,h}$	r_c	$L_{1,uh}$	r_c	$L_{2,h}$	r_c	$L_{2,uh}$
case 1								case 1							
0.324	0.0311	0.355	0.0031	0.291	0.0526	0.308	0.0052	0.961	0.0036	1.019	0.0023	1.016	0.0059	0.924	0.0045
0.523	0.0248	0.493	0.0024	0.575	0.0430	0.485	0.0042	1.063	0.0019	1.079	0.0011	1.040	0.0029	0.929	0.0026
0.586	0.0173	0.601	0.0017	0.613	0.0289	0.659	0.0030	1.066	0.0009	1.084	0.0005	0.974	0.0014	1.170	0.0014
	0.0115		0.0011		0.0189		0.0019		0.0004		0.0003		0.0007		0.0006
case 2								case 2							
0.726	0.0070	0.493	0.00273	0.795	0.0126	0.463	0.0040	1.078	0.0038	1.006	0.0023	0.971	0.0060	0.911	0.0047
0.790	0.0042	0.657	0.00194	0.846	0.0073	0.693	0.0029	1.016	0.0018	1.107	0.0011	1.033	0.0031	1.059	0.0025
1.012	0.0024	0.855	0.00123	1.625	0.0040	0.845	0.0018	1.101	0.0009	1.115	0.0005	1.010	0.0015	1.005	0.0012
	0.0012		0.00068		0.0013		0.0010		0.0004		0.0002		0.0007		0.0006
case 3								case 3							
0.951	0.0039	0.506	0.0027	0.899	0.0065	0.531	0.0038	0.957	0.0043	0.971	0.0009	0.928	0.0076	0.978	0.0016
1.015	0.0020	0.799	0.0019	0.967	0.0035	0.776	0.0026	1.144	0.0022	1.031	0.0005	1.000	0.0040	0.930	0.0008
1.038	0.0010	0.752	0.0011	1.033	0.0018	0.941	0.0015	1.000	0.0010	1.118	0.0002	1.029	0.0020	1.066	0.0004
	0.0005		0.0006		0.0009		0.0008		0.0005		0.0001		0.0010		0.0002
case 4								case 4							
0.930	0.0038	0.548	0.0025	0.902	0.0064	0.582	0.0037	0.900	0.0042	1.064	0.0009	0.866	0.0076	0.943	0.0015
1.000	0.0020	0.768	0.0017	0.950	0.0034	0.835	0.0025	1.003	0.0023	1.070	0.0004	1.057	0.0042	1.007	0.0008
1.000	0.0010	0.977	0.0010	0.986	0.0018	0.929	0.0014	1.111	0.0011	1.014	0.0002	1.003	0.0020	1.061	0.0004
	0.0005		0.0005		0.0009		0.0007		0.0005		0.0001		0.0010		0.0002

Figure S2. Test 1. L_1 and L_2 norms of the relative errors for h and uh . Structured meshes.

Test 2. Rain in a 1D channel

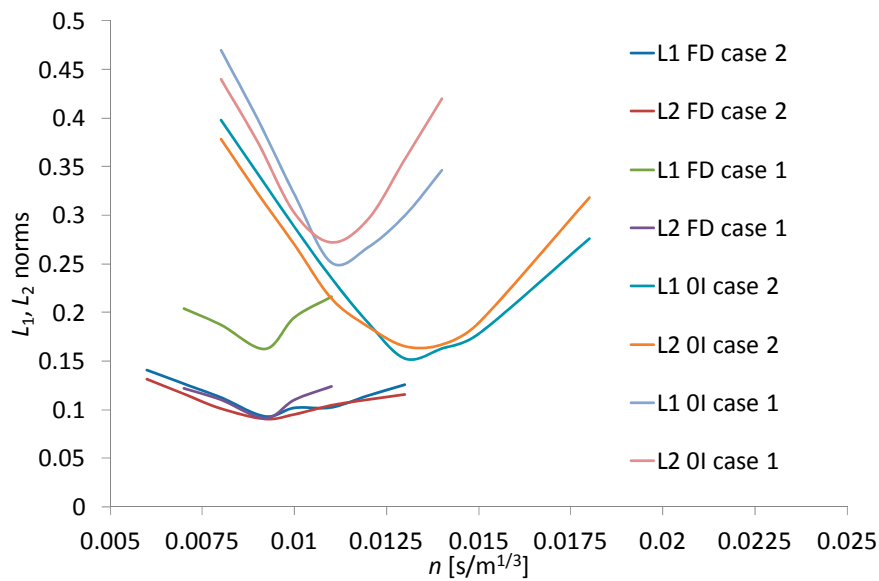


Figure S3. Test 2. L_1 and L_2 norms of q_{out} .

Test 3. Rainfall in a 2D catchment

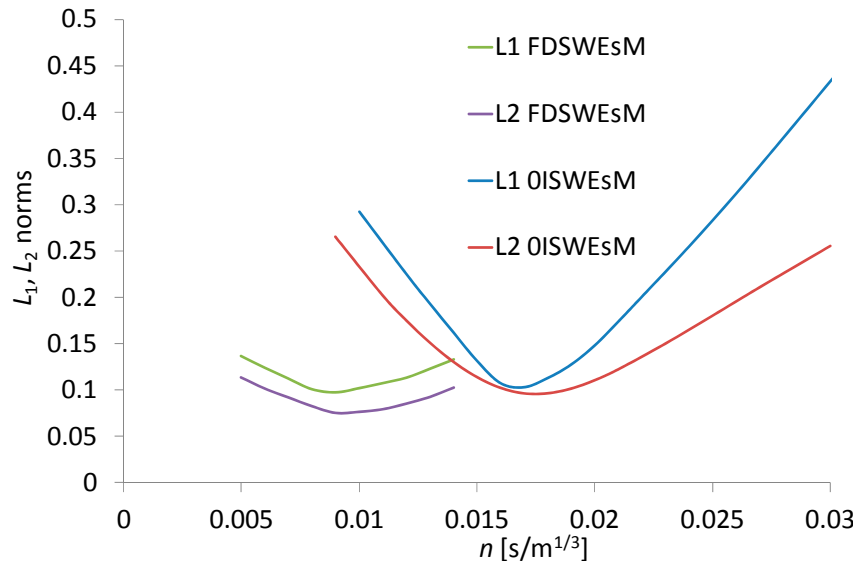


Figure S4. Test 3. L_1 and L_2 norms of q_{out} .

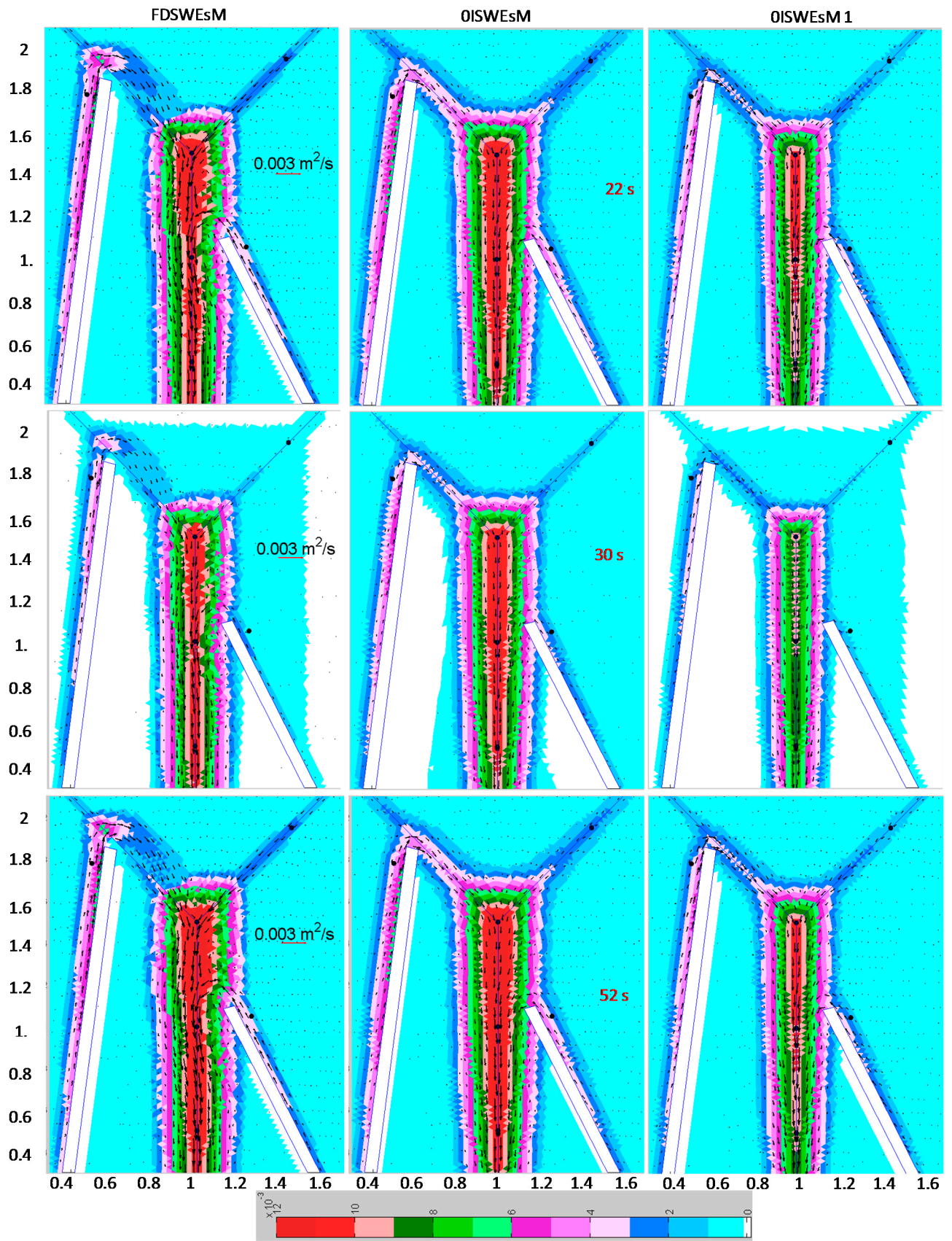


Figure S5. Test 3. Computed water depth and vectors of unitary flow rate at different durations. 22 s (top), 30 s (middle), 52 s (bottom).

Test 4. The Toce river case

Table S1. Test 4. Values of the L_1 , L_2 L_{inf} norms of the relative errors at the gauges [-]

gauge	FDSWEsM n_0			OISWEsM n_0			OISWEsM n_{opt}		
	L_1	L_2	L_{inf}	L_1	L_2	L_{inf}	L_1	L_2	L_{inf}
P1	6.65E-04	8.04E-04	3.65E-02	9.07E-04	1.10E-03	5.96E-02	9.07E-04	1.09E-03	5.83E-02
P2	6.83E-04	9.29E-04	3.97E-02	2.69E-03	2.56E-03	7.34E-02	1.64E-03	1.44E-03	5.25E-02
P3	9.53E-04	8.73E-04	2.09E-02	1.33E-03	1.39E-03	6.25E-02	1.27E-03	1.39E-03	5.95E-02
S4	1.29E-03	1.69E-03	5.59E-02	1.40E-03	1.90E-03	5.08E-02	1.23E-03	1.74E-03	4.60E-02
P4	5.51E-04	1.04E-03	7.59E-02	9.74E-04	1.32E-03	6.64E-02	9.74E-04	1.32E-03	6.64E-02
S6S	4.29E-04	5.66E-04	1.44E-02	3.45E-03	3.95E-03	5.46E-02	2.31E-03	2.99E-03	4.29E-02
S6D	1.12E-03	9.76E-04	2.15E-02	1.49E-03	2.43E-03	3.46E-02	8.78E-04	1.32E-03	3.16E-02
P5	1.23E-03	1.43E-03	4.07E-02	2.71E-03	3.28E-03	6.39E-02	1.64E-03	1.80E-03	5.29E-02
P8	1.53E-03	2.87E-03	4.32E-02	2.46E-03	3.84E-03	7.06E-02	1.54E-03	2.09E-03	6.30E-02
S8D	6.33E-04	8.87E-04	2.30E-02	2.96E-03	4.95E-03	5.42E-02	7.10E-04	9.80E-04	2.70E-02
P9	8.31E-04	1.07E-03	3.96E-02	4.68E-03	7.33E-03	7.90E-02	2.46E-03	3.89E-03	7.63E-02
P10	8.06E-04	1.08E-03	2.69E-02	3.18E-03	6.54E-03	7.89E-02	1.15E-03	1.55E-03	4.45E-02
P12	5.94E-04	8.53E-04	1.70E-02	1.00E-03	1.60E-03	3.91E-02	8.86E-04	1.33E-03	3.91E-02
P13	1.42E-03	2.32E-03	6.75E-02	2.97E-03	5.61E-03	6.92E-02	2.18E-03	3.22E-03	6.75E-02
P18	2.05E-03	3.63E-03	5.80E-02	2.24E-03	3.61E-03	7.97E-02	1.16E-03	1.87E-03	4.87E-02
P19	3.78E-04	7.50E-04	3.00E-02	1.90E-03	2.40E-03	5.57E-02	1.45E-03	1.45E-03	3.88E-02
P21	1.19E-03	1.37E-03	4.17E-02	3.63E-03	7.23E-03	8.14E-02	1.57E-03	2.28E-03	5.39E-02
P23	2.59E-03	2.37E-03	4.95E-02	5.52E-03	8.32E-03	1.35E-01	4.38E-03	5.76E-03	8.41E-02
P24	2.67E-03	2.22E-03	3.53E-02	7.69E-03	1.63E-02	1.80E-01	5.53E-03	9.97E-03	1.38E-01
P25	2.76E-03	2.44E-03	3.62E-02	5.86E-03	1.65E-02	1.86E-01	3.83E-03	8.07E-03	1.07E-01
P26	1.80E-03	2.50E-03	4.53E-02	7.31E-03	8.32E-03	1.69E-01	6.12E-03	6.26E-03	8.35E-02

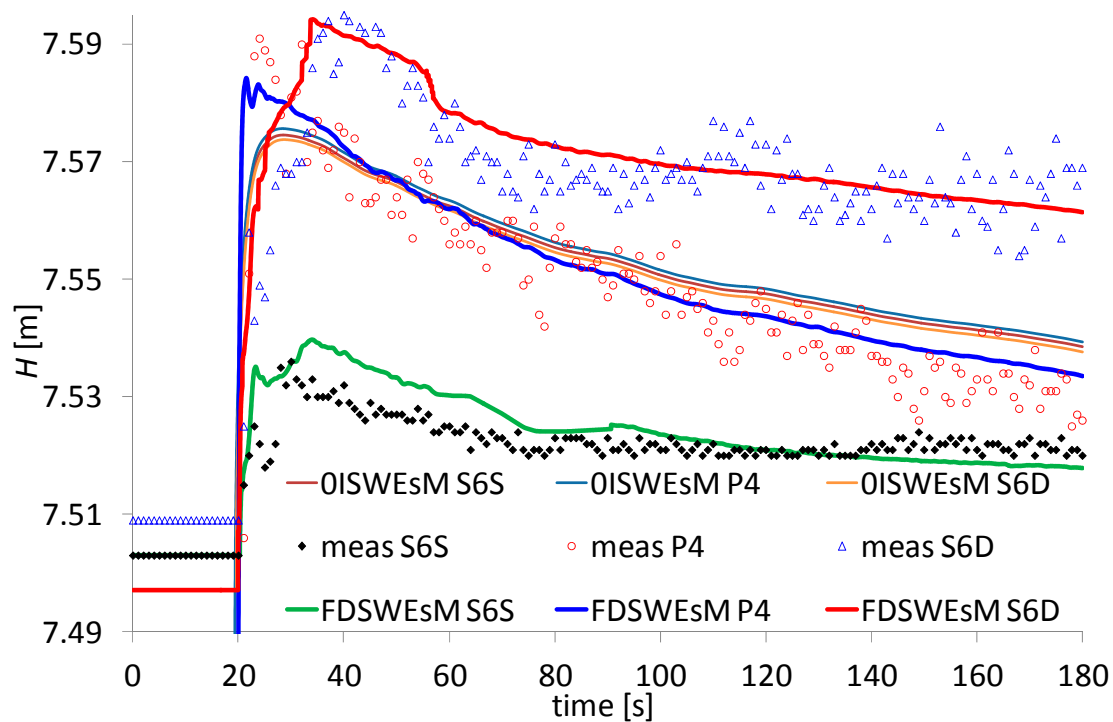


Figure S6. Test 4. Measured and computed water levels at gauges S6S, P4 and S6D.

Reference

1. Aricò, C., Tucciarelli, T. MAST solution of advection problems in irrotational flow fields, *Adv. Wat. Res.* **2007**, *30*, 665–685
2. Aricò, C., Tucciarelli, T. A Marching in space and time (MAST) solver of the shallow water equations. Part I: The 1D case, *Adv. Wat. Res.* **2007**, *30*, 1236–1252
3. Aricò, C., Nasello, C., Tucciarelli, T. A Marching in space and time (MAST) solver of the shallow water equations. Part II: The 2D case, *Adv. Wat. Res.* **2007**, *30*, 1253–1271
4. Aricò, C., Sinagra, M., Begnudelli, L., Tucciarelli, T. MAST-2D diffusive model for flood prediction on domains with triangular Delaunay unstructured meshes, *Adv. Wat. Res.* **2011**, *34*, 1427–1449
5. Aricò, C., Sinagra, M., Tucciarelli, T. MAST solution of “anisotropic” flow problems: application to the shallow water equations, *Adv. Wat. Res.* **2013**, *62*, 13–36
6. Aricò, C., Lo Re, C. A non-hydrostatic pressure distribution solver for the nonlinear shallow water equations over irregular topography, *Adv. Wat. Res.* **2016**, *98*, 47–69
7. Bermúdez, A., Vázquez, M.E., Upwind methods for hyperbolic conservation laws with source terms, *Comput. Fluids*, **1994**, *23*, 1049–1071